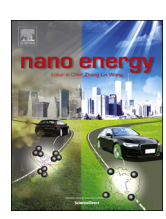
FISEVIER

Contents lists available at ScienceDirect

Nano Energy

journal homepage: www.elsevier.com/locate/nanoen



Communication

A robust 2D organic polysulfane nanosheet with grafted polycyclic sulfur for highly reversible and durable lithium-organosulfur batteries



Hao Hu^{a,b,1}, Bote Zhao^{a,1}, Haoyan Cheng^b, Shuge Dai^a, Nicholas Kane^a, Ying Yu^{b,*}, Meilin Liu^{a,*}

- ^a School of Materials Science and Engineering, Georgia Institute of Technology, Atlanta, GA 30332-0245, USA
- b Institute of Nano-science and Nano-technology, College of Physical Science and Technology, Central China Normal University, Wuhan, Hubei 430079, PR China

ARTICLE INFO

Keywords: Organic polysulfane Polymer nanosheet Surface enhanced Raman scattering Lithium-organosulfur battery

ABSTRACT

Organic polysulfanes are new type of attractive organosulfur electrode materials for next generation lithium-sulfur (Li-S) batteries because of their high sulfur content, low cost, and desirable energy density. However, conventional organic polysulfanes usually suffer from poor reversibility due to structure variation and irreversible conversion during cycling. Here we report the synthesis and characterization of a novel two-dimensional (2D) organic polysulfane with a unique molecular structure of polycyclic sulfur directly substituting the carboxyls of poly(acrylic acid) and grafted on the carbon chain through a coupling reaction with KI as a catalyst and KCl as a template. The obtained organic polysulfane nanosheets with 72 wt% sulfur (OPNS-72) exhibit high initial capacity of 891 mAh/g (based on whole composite), excellent cycling stability (0.014% capacity fading per cycle over 620 cycles at 1 C rate), superior rate capability (562 mAh/g at 10 C) and high mass loading of 9.7 mg/cm². The remarkable cycling stability of the Li-S battery is attributed to the structural stability and highly reversible electrochemical reaction of the OPNS-72 electrode, as confirmed by the TEM image after cycling and operando Raman spectroscopy measurements under battery operating conditions. Further, the developed synthesis approach is applicable for the preparation of other organic polysulfane nanosheets as highly reversible electrodes for Li-S batteries.

1. Introduction

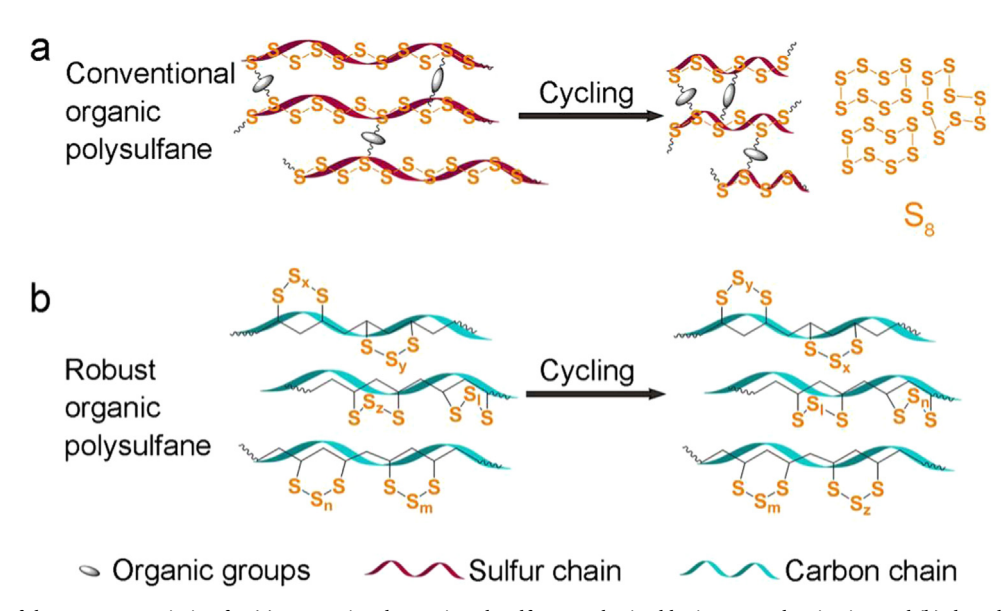
Lithium-sulfur (Li-S) batteries have received significant attention during the past decade due to the low cost of elemental sulfur, and high theoretical specific capacity of the sulfur cathode [1-3]. However, the commercial application of Li-S batteries is still hindered by the dissolution and shuttling effect of long chain lithium polysulfides (Li₂S₄₋₈), which always lead to poor cycling performance and limited rate capability [4-6]. To restrain shuttling effect during cycling without compromising the capacity and durability, the composition, structure, and morphology of the sulfur-based electrode materials must be carefully designed. One strategy is creating hybrid sulfur-based composites, such as introducing functional organic materials, transition metal oxides, and noble-metals to contain sulfur, or exploiting structured carbon/ polymer as multilayer barrier to restrain polysulfides [1]. Despite the extensive usage of these strategies, they often involve complicated synthesis processes and harsh synthesis conditions to achieve desired adsorption between metal oxides/carbon matrices and polysulfides [7,8]. Moreover, the obtained electrode materials are always suffering from a significant expansion of the electrode volume, resulting in decreased volumetric/gravimetric energy density of Li-S batteries [9–12].

Another effective strategy for restraining the shuttling effects is preparing sulfur-rich organic materials (organic polysulfanes), which is a class of polymers with alternating chains of sulfur and hydrocarbons. They are promising organosulfur electrode candidates for Li-S batteries due to their unique structure and natural attractive polysulfide adsorption ability [4,13–15]. Moreover, organic polysulfanes can achieve high sulfur loading and hence high capacity. Currently, inverse vulcanization is the most common method to prepare sulfur-rich organic polysulfanes. Briefly, polymeric sulfur chains are prepared by using elemental sulfur as a feedstock, and then organic groups (alkyl or aryl) are used as connectors to link the polymeric sulfur chains via carbon atoms to form an R-S_n-R type copolymer [16]. However, the use of this type of organic polysulfane as an electrode material encounter several drawbacks: (i) the polymeric sulfur chains are unstable and they always break up during discharge process [14], resulting in poor mechanical properties and bad stability. (ii) The large volume change (≈ 80%) of these organic polysulfanes during charge and discharge cycles are

^{*} Corresponding authors.

E-mail addresses: yuying01@mail.ccnu.edu.cn (Y. Yu), meilin.liu@mse.gatech.edu (M. Liu).

¹ These authors contributed equally to this work.



Scheme 1. Schematic of the structure variation for (a) conventional organic polysulfane synthesized by inverse vulcanization and (b) the robust organic polysulfane with polycyclic sulfur grafted on the carbon chain of a PAA (in this work) before and after lithiation/delithiation cycles.

always accompanied by an irreversible conversion of the electrode materials from homogeneous sulfur-rich organic polysulfanes to heterogeneous sulfur-lean organic polysulfanes and elemental sulfur (Scheme 1a) [17]. This irreversible conversion causes inevitable loss of sulfur and structure variation, leading to low coulombic efficiency and poor cycle life [14,17].

In addition to the inverse vulcanization, there are other alternative vulcanization strategies, including using addition reaction between elemental sulfur and a polymer with alkyl or aryl functional groups, and substitution reaction between thiol-based materials and a polymer with halogen or carboxyl functional groups to form C-S bonds [8,15]. This kind of product can be considered as a class of sulfur doped-polymers. The carbon chain in these flexible polymers with good stability can potentially buffer the volume variation during cycling. However, this vulcanization strategy is yet to be used for preparation of sulfur electrodes due to the relatively low sulfur content and uncontrollable morphology of the final product [18]. Thus, it is highly desirable to use this vulcanization strategy for synthesis of a chemically stable polymer with a controllable morphology and high sulfur content.

Herein we report our findings in the synthesis of a new kind of organic polysulfane nanosheets (OPNS) with high sulfur content (up to 93 wt% sulfur) using poly(acrylic acid) (PAA) and sulfur nanospheres as raw materials, where sulfur directly grafts on the carbon frame of PAA through direct coupling reactions initiated with decarboxylation of PAA. The coupling reaction that presents high selectivity may efficiently suppress the side reactions [19,20] and it is a convenient method to achieve sulfur-rich compounds. Moreover, the coupling reactions can be performed in the solid phase, which does not require harsh reaction conditions, expensive materials, or special solvents. The final products not only retain the desirable electrochemical activity of elemental sulfur, but also present improved electrochemical performance as a result of the nanosheet morphology. Compared with the structure of conventional organic polysulfane synthesized by inverse vulcanization (Scheme 1a), the structure of our organic polysulfane with polycyclic sulfur grafted on the carbon chain of PAA (Scheme 1b) possesses the advantages of the stability during lithiation/delithiation cycling. Specifically, the OPNS cathodes for Li-S batteries demonstrated excellent rate performance (562 mAh/g at 10 C) and high initial capacity 891 mAh/g at 1 C rate (based on the mass of organic polysulfane), together with only 0.014% capacity fading per cycle over 620 cycles. Additionally, this facile and solvent-free method can be easily scaled up while maintaining the high purity of the final products.

2. Experimental section

2.1. Chemicals and materials

Bulk sulfur (S, 99.98%), ethylenediamine (99.5%), ethanol (99.5%, anhydrous), poly(vinyl pyrrolidone) (PVP, MW \approx 4,0000), acetic acid (99.7%), poly(acrylic acid) (PAA, MW \approx 130,000), potassium iodide (KI, 99.5%), potassium chloride (KCl, 99.0%), were all obtained from Sigma-Aldrich (St. Louis, MO) and used without further purification. Deionized water (18.2 M Ω cm) obtained by purification through a Milli-Q system (Millipore, USA) was used throughout the experiments.

2.2. Synthesis of sulfur nanospheres

The 2D organic polysulfane nanosheets were prepared by PAA and sulfur nanospheres. Since bulk sulfur does not mix well with PAA, sulfur nanospheres were prepared to facilitate mixing with PAA. In the typical synthesis process, 0.2 g of bulk sulfur powders were added to a 20 mL of the solution composed of ethylenediamine and ethanol (1:1, vol: vol), which was stirred at room temperature (21 °C) for 10 h to form a homogeneous reddish-brown solution. Then the solution was slowly dropped into 500 mL of PVP aqueous solution (0.1 wt%) under stirring. The color of the solution changed from colorless to bright orange. After 5 h, a 7.5 mL of acetic acid was slowly dropped into the mixed solution. During this process, the color of the solution gradually changed to ricewhite, indicating the neutralization reaction of ethylenediamine and acetic acid. After reaction for 0.5 h, the products were washed three times with deionized water by centrifugation at 11,000 r.p.m. for 15 min to remove the excess precursor and PVP. Finally, sulfur nanospheres with an average size of 172 \pm 23 nm (Fig. S1) were obtained after being dried in a vacuum oven at 60 °C overnight.

2.3. Synthesis of organic polysulfane nanosheets (OPNS)

The OPNS was prepared through direct coupling reactions by the decarboxylation of PAA and substitution with sulfur. In a typical procedure, 0.1 g of PAA, 0.1 g of KI and 0.4 g of sulfur nanospheres were dispersed in a 10 mL solution with deionized water (3 mL) and ethanol (7 mL) to obtain a homogeneous suspension at room temperature (21 °C). 100 g of KCl was mixed with above suspension, and dried at 60 °C under mechanical stirring. To perform the direct coupling reaction, the mixture was then put in a tube furnace at 260 °C for 1–24 h

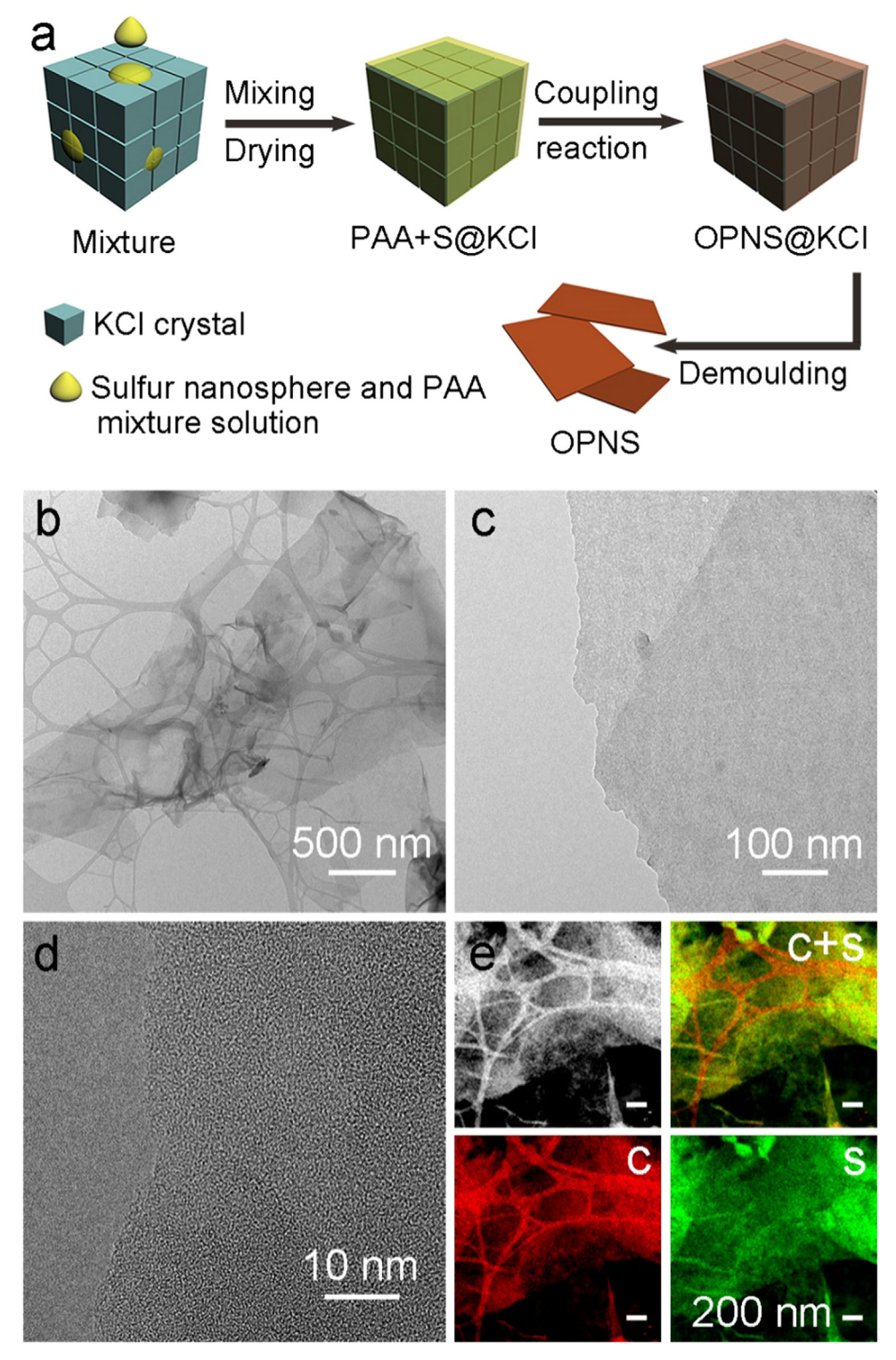


Fig. 1. (a) Schematic of synthetic procedure for organic polysulfane nanosheets (OPNS). (b, c) TEM images of OPNS-72 prepared at 260 °C for 8 h with KI as a catalyst and KCl as a template. (d) HRTEM image of OPNS-72, and (e) STEM image of OPNS-72 and corresponding elemental mapping of C and S in OPNS-72 with the merged mapping also shown.

under argon flowing at 60 sccm. The content of active sulfur in the final product would be decreased with increasing the thermal treatment time. The mixture product after reaction was stirred in ethanol overnight, followed by ultrasonic treatment for 2 h. Then the suspension was washed with ethanol and DI water by centrifugation (11,000 r.p.m. for 15 min) for six times in total. Afterwards, the products were collected after drying under vacuum at 60 °C for 8 h. According to the TGA

curves, the content of active sulfur was calculated to be 93 wt%, 80 wt %, 72 wt%, 50 wt%, and 0 wt% for the products prepared at 260 °C for 1 h, 5 h, 8 h, 12 h and 24 h, respectively. The final products were denoted as OPNS-80, OPNS-72, OPNS-50, and OPNS-0 based on the content of sulfur.

2.4. Basic characterizations

The morphology and micro-structure of the as-prepared samples were characterized by using a transmission electron microscope (TEM) (Hitachi-HT7700, Tokyo, Japan) operated at 120 kV. High-resolution TEM, HAADF-STEM, and EDS mapping analyses were all performed at 200 kV using a JEOL ARM200F microscope (JEOL, Tokyo, Japan) with STEM aberration corrector. Conventional XRD patterns were recorded using an X'Pert PRO Alpha-1 diffractometer (PANalytical, Almelo, The Netherlands). The specific surface areas were determined by the Brunauer-Emmett-Teller (BET) method using the adsorption branch with a Micromeritics ASAP 2020 surface area/porosity analyzer, FTIR spectrum was recorded using an FTIR spectrometer (Nicolet iS50 FT-IR. American) in the range of 400-2000 cm⁻¹. Raman spectrum were recorded at room temperature using a Renishaw RM 1000 spectro-microscopy system used He-Ne laser (Thorlabs HRP-170) at 632.8 nm wavelength. For the in-operando Raman test, the cell was assembled using OPNS-72 (0.3 mg/cm²) as the cathode, Li foil as the anode and glass filter paper (Whatman, GF/F) as the separator with 120 µL of electrolyte. The stainless steel test cell was used as we reported previously [21]. In-operando Raman spectra of OPNS-72 were taken at various cell voltages by applying a CV sweep between 3.0 and 1.5 V at a rate of 0.1 mV/s.

2.5. Electrochemical measurements

Electrochemical measurements were performed using two electrode Swagelok cells with Li foil as both the counter and reference electrodes at ambient temperature. Consideration of the poor conductivity (inherit from sulfur) and good cohesiveness (derived from PAA) of the organic polysulfane, the working electrode consisted of active material (70 wt %), conductivity agent (carbon black, Super-P, 20 wt%), and polymer binder (PVDF, 10 wt%) with NMP as slurry dispersant and aluminum foil as current connecter. The OPNS mass loading in electrodes for CV and cycling testing were 1.1-9.7 mg/cm². The electrolyte consisted of 1 M LiN(CF₃SO₂)₂ and 0.1 M anhydrous lithium nitrate in a mixed solvent of 1,3-dioxolane and dimethyl ether (1:1, vol: vol). The cells were assembled in an argon-filled glove box. Galvanostatic chargedischarge tests were performed using a Neware (CT2001A, China) battery testing system between 1.7 and 2.7 V (vs. Li/Li⁺). Before testing, the cells were aged for 12 h. The cyclic voltammetry (CV) curve was recorded between 1.5 and 3.0 V by an electrochemical work station (PARSTAT 2273, Princeton Applied Research, USA).

3. Results and discussion

3.1. Synthesis of sulfur-rich organic polysulfane nanosheets (OPNS)

To minimize the lithium diffusion length and improve the conductivity of sulfur-based polymers, periodic or porous templates were widely used to increase the specific surface area of organic polysulfane cathodes [8,13-15]. However, these strategies were highly limited by the poor fluidity of organic polysulfane. Here, we introduce KCl template in the precursor to form ultra-thin organic polysulfane nanosheet. Water-soluble, self-stacking KCl crystals, which were widely used as a template to prepare transition metal oxide nanosheets [22], were not only used as the hard template for the precursor to form OPNS but also acted as diluent to avoid the aggregation of melted sulfur to form independent sulfur particles. The schematic of synthetic procedure for organic polysulfane nanosheets (OPNS) was show in Fig. 1a. TEM images of sulfur-rich organic polysulfane nanosheets prepared after thermal treatment at 260 °C for 8 h with the assistance of KI and KCl (denoted as OPNS-72, see the Experimental section for details) are shown in Fig. 1b-d. The ultrathin nanosheets show an average size of 2–3 μm (Fig. 1b and Fig. 1c). No obvious lattice fringe can be found in the high-resolution TEM images in Fig. 1d, suggesting disordered

arrangement of sulfur and carbon atoms [23]. Even though sulfur nanospheres were used as feedstock to prepare the OPNS-72, no sulfur aggregation or particles were observed in the final product, indicating the sulfur completely reacted with PAA during the coupling reaction. The scanning transmission electron microscopy (STEM) and corresponding elemental mapping (C, S) in Fig. 1e graphically reveal the uniform distributions of C and S. XRD spectra of OPNS-72 and sulfur nanospheres are shown in Fig. S2. The broad peak of OPNS-72 centered between 20 and 30° implied the amorphous structure [24-26] of prepared organic polysulfane. In addition, there were no characteristic peaks of elemental sulfur in the spectrum of OPNS-72, indicating the absence of aggregated sulfur particles, which was consistent with the TEM observations in Fig. 1b-d. In the synthesis process, KCl was used as a hard template to create the two-dimensional (2D) microstructure of organic polysulfane, thereby avoiding the aggregation of products during thermal treatment at high temperature. Such ultra-thin 2D materials have attracted much attention in energy storage because of the highly exposed electrochemical active surface to the electrolyte and facilitated ion/electron transfer [9,22,27], resulting in high electrochemical performance. According to analysis of N2 adsorption-desorption isotherm (Fig. S3a), the OPNS-72 had a high specific surface area of 224 m²/g, further evidenced the structural advantage of the 2D organic polysulfane prepared with the assistance of a KCl template. In the case without KCl, the obtained products gathered together, forming agglomeration (Fig. S4), resulting in a very low specific surface area of 5 m²/g (Fig. S3b). Thus, the KCl template plays an important role in creating the 2D structure of the polymer, and also clearly demonstrates the promise of such salt-template in the synthesis of 2D polymers.

It is known that sulfur radicals are very important for the incorporation of elemental sulfur into polymers, which could enable an addition reaction between elemental sulfur and a polymer or a polymerization reaction between elemental sulfur and dialkene or dialkyne monomoleculars [15,16], forming organic polysulfanes. For pure PAA, the decarboxylation can be achieved when the temperature was above 383 °C (Fig. S5a). This temperature is much higher than the sublimation temperature of elemental sulfur (308 °C, Fig. S5b). Fortunately, we found that the existence of sulfur radicals could efficiently execute the decarboxylation of PAA at a low temperature of 260 °C (Fig. 2a). At 260 °C, the coupling reaction between sulfur radicals and PAA occurred quickly, accompanied by a rapid color change of the products from rice yellow to black (Fig. S6). Previous researches have shown alkali halides can effectively promote the ring opening of S₈ and generation of sulfur radicals [19]. In this research, KI was introduced here to increase the quantity of sulfur radicals followed by an electron-transfer pathway for the reduction of S_8 to di- or tri-sulfur monoradicals and the reaction as following [28]:

$$S_8 + 4I^- \leftrightarrow 4S_2^{\bullet-} + 2I_2 \tag{1}$$

$$3S_8 + 8I^- \leftrightarrow 8S_3^{*-} + 4I_2$$
 (2)

The as-generated I2 can be easily vaporized at 260 °C, and the residual KI can be easily removed by deionized water after the reaction. With the assistance of KI and high temperature (260 °C), abundant sulfur radicals were formed to promote the coupling reaction with PAA. The content of the sulfur in OPNS can be controlled from 93 wt% to 0 wt% (determined by TGA in Fig. S7a-e) by prolong reaction time from 1 to 24 h (Fig. 2b). Specifically, the content of sulfur was 80 wt%, 72 wt %, 50 wt% and 0 wt% when the reaction time was 5 h, 8 h, 12 h, and 24 h, respectively (Fig. S7b-e). The corresponding samples were denoted as OPNS-80, OPNS-72, OPNS-50, and OPNS-0, respectively, where the numbers represent the weight percentage of sulfur in the samples. By contrast, the content of sulfur in the sample prepared without the assistance of KI was much less under the same synthetic conditions (reaction at 260 °C for 5 h, with KCl as a template) (Fig. S7f). The sulfur content differed by approximately 2.4 times (with KI: 80 wt %; without KI: 32 wt%), indicating the importance of KI as a catalyst in

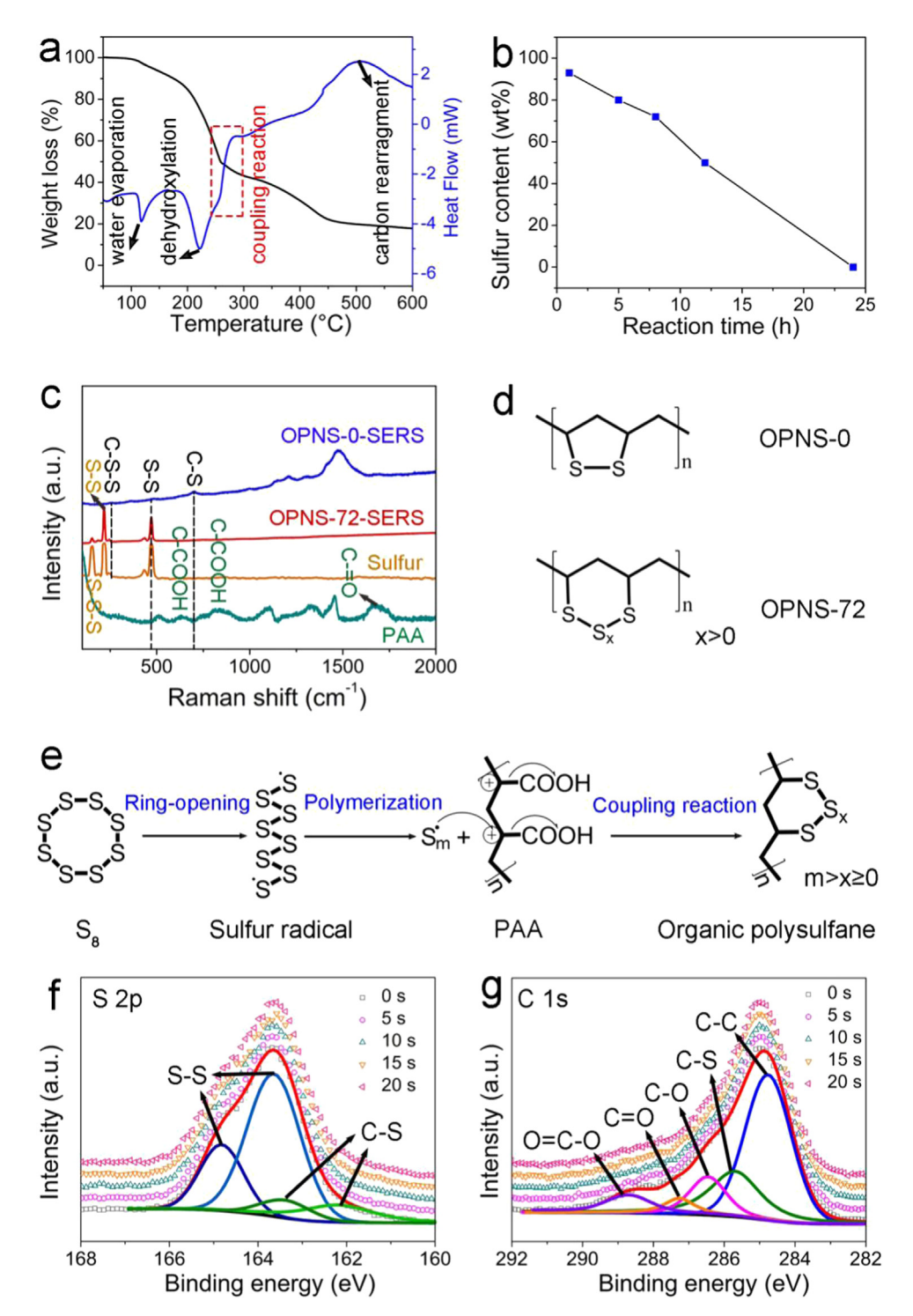


Fig. 2. (a) TGA and DSC curves of PAA and sulfur nanosphere mixture (with a mass ratio of 1:4) under argon flow. (b) The relationship between coupling reaction time and sulfur content in OPNS. (c) Raman spectra of PAA and sulfur nanospheres and surface enhanced Raman scattering (SERS) spectra of OPNS-72 (OPNS-72-SERS) and OPNS-0 (OPNS-0-SERS), (d) the molecular structure of OPNS-0 and OPNS-72. (e) The schematic diagram of synthesis mechanism for the proposed organic polysulfane, (f) S 2p and (g) C 1s XPS spectra of OPNS-72.

the coupling reaction.

3.2. Understanding the molecular structure of OPNS and formation mechanism

The molecular structure of OPNS-72 was investigated by surface enhanced Raman scattering (SERS). It was reported that Ag nanocubes with sharp corners and edges could enhance the Raman scattering cross section by 10^7 – 10^8 -fold in terms of enhancement factor [29,30]. There

are no observable peaks of sulfur or PAA in the Raman spectra of OPNS-72 and OPNS-0 without application of SERS (Fig. S8). In contrast, with the assistance of 65 \pm 5 nm Ag nanocubes (Fig. S9), there are obvious characteristic peaks in the Raman spectrum of OPNS-72 (noted as OPNS-72-SERS) in Fig. 2c. Compared with PAA, the characteristic band of C-COOH located at 634, 842 cm $^{-1}$ and C=O stretch at 1681 cm $^{-1}$ disappeared [31,32], indicating the decarboxylation of PAA during thermal treatment with sulfur. Specifically, for the OPNS-72-SERS, the peak at 753 and 271 cm $^{-1}$ signify bending of the C-S and C-S-S [16,19],

confirming the coupling reaction happened between PAA and sulfur. While the other two characteristic vibrational bands at 487 (S-S bend) and 171 cm⁻¹ (S-S-S bend) [14,16] demonstrate the existence of sulfur chains (Sx) in OPNS-72-SERS. To get rid of the influence from sulfur chain, we also investigated the SERS spectrum of the OPNS-0 (OPNS-0-SERS), which was prepared after thermal treatment at 260 °C for 24 h under argon flow. Compared with OPNS-72-SERS, the characteristic peak of the S-S-S bend located at 171 cm⁻¹ disappeared, indicating the breaking of the sulfur-chain during long time of thermal treatment. The detailed peak information for PAA and the SERS spectrum of the OPNS-0-SERS can be further seen in Fig. S10. Specifically, the peaks at 1138 and 1011 cm⁻¹ signify the symmetrical and asymmetrical stretching modes for C-C while the peaks at 1211, 1307, and 1476 cm⁻¹ can be assigned to the twist bend, wag bend, and deformation stretching modes of -CH2 groups [31], respectively. The weak peaks at 619 and 1413 cm⁻¹ are the out-plane bending mode and deformation of -CH [24,26]. All these peaks implied that the OPNS-0 retained the carbon chain of PAA. Considering all characteristic peaks in the Raman spectra, a logical molecular structure of OPNS-0 and OPNS-72 can be proposed in Fig. 2d. Considering the sulfur content in the OPNS-0 sample was 0 wt% based on the TGA result, it is indicated that the carbon connected sulfur can not be detected by the TGA. On the basis of the above analysis, the detailed formation mechanism of organic polysulfane nanosheets was proposed (Fig. 2e). A synergetic effect of high temperature (260 °C) and a sulfur radical trapper (KI) result in equilibrium ringopening of the S₈ monomer into linear sulfur radical, which subsequently polymerizes into polymeric sulfur radical (Sm*) with high molecular weight. The S_m could further catalyze the decarboxylation of PAA and substitute the carboxyl groups in PAA though the coupling reaction, forming multi-sulfur-grafted organic polysulfanes.

The chemical state of the prepared organic polysulfane was further investigated by X-ray photoelectron spectroscopy (XPS). The XPS spectra of the OPNS-72 confirmed the presence of sulfur in OPNS-72 (Fig. 2f and g). Except for the typical doublet of S 2p_{3/2} and 2p_{1/2} (163.7 and 164.9 eV) in Fig. 2f for S-S bond with an energy separation of 1.2 eV, the individual peak located at 262.5 eV reconfirmed the presence of C-S bonds [27]. Moreover, the binding energy of the S 2p_{3/2} peak for S-S (163.7 eV) in OPNS-72 is lower than that of elemental sulfur (164.0 eV) [8], which was ascribed to the influence of carbon chain. Compared with the C 1s XPS spectrum of carbon black (Fig. S11), the C-S bond was detected around 285.5 eV in C 1s spectrum of OPNS-72 (Fig. 2g), which is closest to the C-C bond at 284.7 eV [33,34]. Moreover, the peak's area ratio of C1s for C-C and C-S in OPNS-72 was calculated to be 2:1, revealing the substitution of the carboxyl groups in PAA by sulfur. The presence of O in the XPS results were derived from adsorbed gas and water. These XPS spectra did not change under the prolonged X-ray etching time, suggesting the homogenous structure of OPNS-72. Moreover, the Fourier transform infrared (FT-IR) spectrum in Fig. S12 indicated that the OPNS-72 has inherited the carbon chain of the PAA and the sulfur has been successfully grafted to this carbon frame. All the above results further support the proposed formation mechanism of organic polysulfane in Fig. 2e. And the sulfur content in OPNS measured by TG should just include these non-carbon connected sulfur (S_v).

3.3. Electrochemical performance and lithium storage mechanism analysis of OPNS cathode

The electrochemical properties of organic polysulfane cathodes with different sulfur content (50 wt%, 72 wt%, and 80 wt%) were evaluated in a test cell using Li foil as the anode. Fig. 3a show the initial discharge/charge curves within a voltage window of 1.7–2.7 V (versus Li $^+$ /Li) at 1 C rate (1 C = 1670 mA/g_s). Two distinct plateaus at 2.3 and 2.0 V (vs. Li/Li $^+$) shown in the first discharge curve (Fig. 3a) were associated with sulfur reduction and formation of long chain polysulfides (S_{1–4} 2) and short chain polysulfides (S_{1–4} 2) [35,36],

respectively. During the subsequent charge process, in addition to the conversion of $\text{Li}_2\text{S}_2/\text{Li}_2\text{S}$ to lithium polysulfides at 2.3 V, another charge plateau at 2.5 V can be possibly attributed to further oxidation [37]. As expected, the electrode with higher sulfur content in OPNS displayed higher charge-transfer resistance (Fig. S13), due likely to poor electronic conductivity. It is also noted that OPNS-80 (with more sulfur content compared with OPNS-50 and OPNS-72) showed slower lithium diffusion, as reflected by the smaller slope of the impedance arc in the low frequency range. The high initial coulombic efficiencies of OPNS-50 (98%) and OPNS-72 (98%) implied limited diffusion of polysulfides in the cycling process, which is attributed to OPNS's strong adsorption of dissolvable lithium polysulfide such as Li₂S₆ (Fig. S14). The initial coulombic efficiency of 107% for the OPNS-80 electrode is attributed to the side reaction during the discharge process. In the Li-S battery, the irreversible Li₂S could be easily formed during the discharge process when using a nanostructured cathode, which would lead to a large potential barrier for the subsequent charge process [38-40]. The amount of as-formed Li₂S depends sensitively on the sulfur content in the electrode materials. For the OPNS-80, the excess sulfur may potentially lead to the formation of more irreversible Li₂S, thus resulting in higher coulombic efficiency than that of OPNS-50 and OPNS-72.

Among all the OPNS composites (Fig. 3b), OPNS-72 exhibits the best cycling performance. OPNS-50 shows poor initial capacity (468 mAh/g, based upon the mass of polysulfanes) at 1 C, but good capacity retention of 98%. While OPNS-80 presented a high initial capacity (1013 mAh/g) but relatively remained low capacity retention of 72% after 200 cycles. In order to further illustrate the contribution of carbon frame in the OPNS-50, OPNS-72 and OPNS-80, the cycling performance of OPNS-0 under the same condition (between 1.7 and 2.7 V at 1 C) was tested. The result in Fig. S15a displayed a poor capacity (63 mAh/g). Further evidence suggested that the redox peak of OPNS-0 electrode was below 1.5 V in the CV curve (Fig. S15b). This result indicated that the carbon-connected sulfur made negligible contribution to the capacity under this test condition.

The charge/discharge capacities of OPNS cathodes with different sulfur content were cycled at various rates with results shown in Fig. 3c. OPNS-80 displayed high initial capacity but poor rate capability, while the OPNS-50 had a lower initial capacity but better rate capability. The rate performance of the OPNS-72 cathode was better than other OPNS cathodes. Specifically, the reversible capacities of OPNS-72 were 889, 840, 686, 643, and 562 mAh/g at 1, 3, 5, 8 and 10 C, respectively. By decreasing the C-rate from 10 C back to 1 C after the cycling test at various rates of 1-10 C, the specific capacity of OPNS-72 could recover to the initial value, indicating the highly reversible lithium storage in the OPNS-72 electrode. As confirmed by elemental mapping of S (Fig. 1e) and molecular structure of OPNS-72 (Fig. 2d), the sulfur clusters were grafted on carbon chain with high dispersity, which was propitious to the diffusion of lithium ions and electrons. This character is responsible for the outstanding rate performance of OPNS-72 over most of other sulfur-based cathodes reported in Li-S batteries (Fig. 3d) [4,8,11,13,41-46]. To characterize the electrochemical behavior of OPNS-72 at high cycling rates, we acquired CV curves of OPNS-72 at different scan rates (Fig. S16). As the scan rate increased from 0.2 to 1.5 mV/s, the area of the reduction peaks for the long chain polysulfides $(S_{4-8}^{2}, 2.3 \text{ V})$ increased significantly, even stronger than that of the short chain polysulfides $(S_{1-4}^{2-}, 2.0 \text{ V})$, suggesting that the long chain polysulfides may have higher activity than the short chain polysulfides and play an important role at high rates. In addition, with the increased scanning rate, both the oxidation peaks and first reduction peaks (around 2.3 V) shift due to the increased polarization. The second reduction peaks around 1.9 V shift to the right, which was caused by the incomplete reduction of polysulfide. Fig. 3e reveals the high cycling performance of OPNS-72 with different mass loading. The electrode with 1.1 mg/cm² shows outstanding initial capacity up to 891 mAh/g at 1 C rate (based on the mass of organic polysulfane), which is slightly higher than the initial capacity of the electrode with a mass loading of

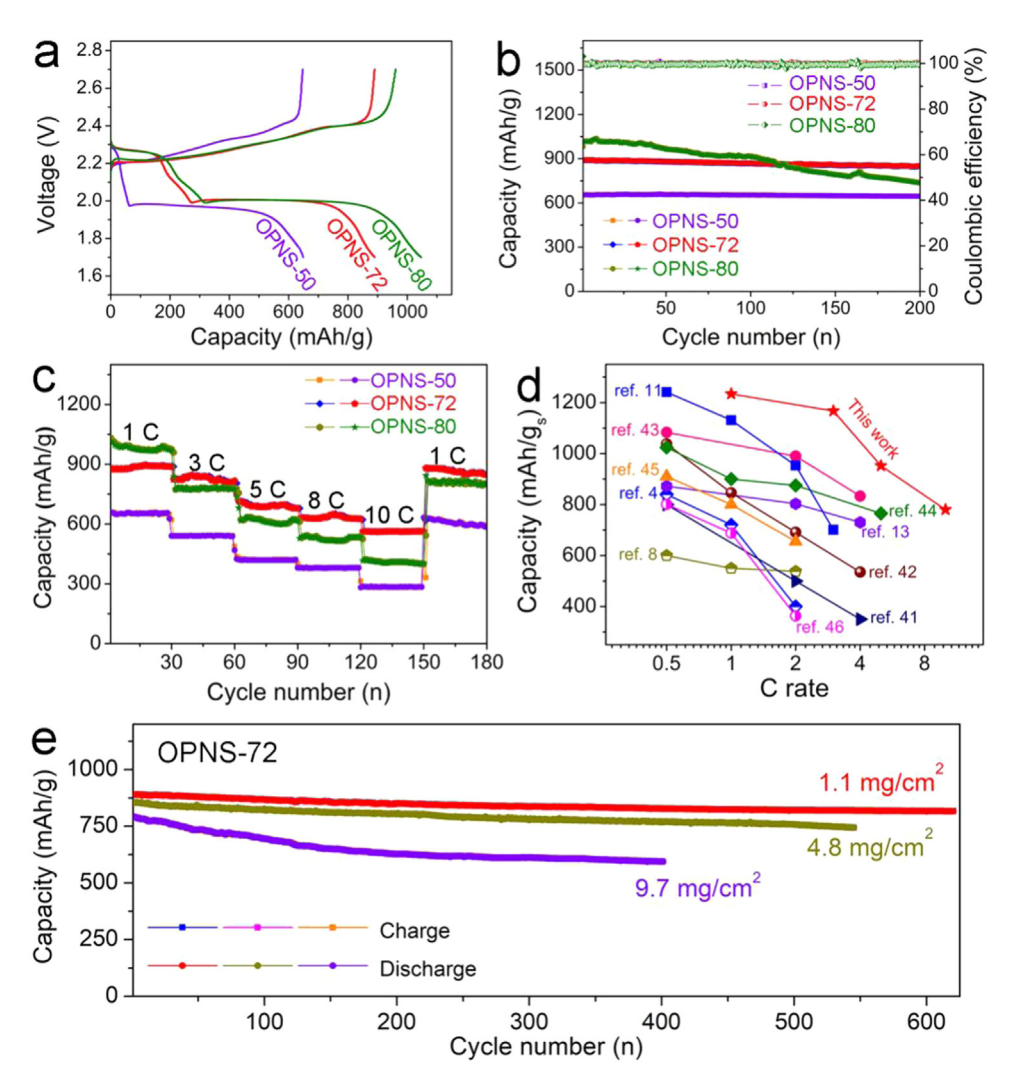


Fig. 3. (a) Initial voltage profiles of galvanostatic discharge/charge curves and (b) cycling performance of OPNS-50, OPNS-72 and OPNS-80 at 1 C (1 C = 1670 mA/g_s) within a voltage window of 1.7–2.7 V. (c) Rate performance of the OPNS-50, OPNS-72 and OPNS-80 within a voltage window of 1.7–2.7 V. The mass loading for the electrolytes in a-c is 1.1 mg/cm². (d) Comparison of the rate performance (based on the mass of sulfur) of the robust polysulfane electrodes (OPNS-72) in this work and other S-based cathodes recently reported. (e) Cycling performance of OPNS-72 with different mass loading at 1 C (1 C = 1670 mA/g_s) within a voltage window of 1.7–2.7 V.

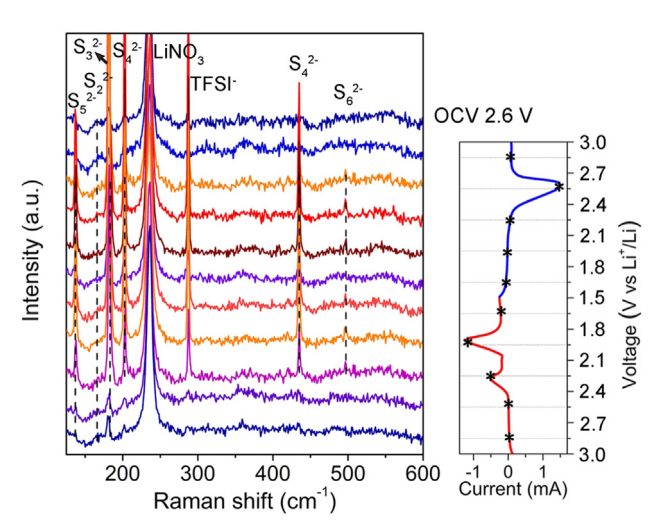


Fig. 4. *In-operando* Raman spectra of a Li-S cell with OPNS-72 as cathode at various voltages (*), and the corresponding voltages were marked on the CV profile during the *in-operando* Raman cycling experiment.

 4.8 mg/cm^2 (855 mAh/g) and 9.7 mg/cm^2 (792 mAh/g). After 620 cycles, a capacity of 811 mAh/g was still maintained for the OPNS-72 electrode (1.1 mg/cm^2), with only 0.014% capacity fading per cycle (91% capacity retention). The reversible capacity of electrode with a higher mass loading of 4.8 mg/cm^2 can be as high as 743 mAh/g after

550 cycles, demonstrating the excellent durability of the obtained OPNS-72. Moreover, the electrode (4.8 mg/cm²) with a high compacted density of 1.38 g/cm³ exhibited high rate capability with high discharge volumetric capacities of 1245 (0.5 C), 1180 (1 C), 1067 (3 C), and 790 (5 C) mAh/cm³ (Fig. S17). In addition, the reversible capacity of electrode with a mass loading of 9.7 mg/cm² after 400 cycles is 594 mAh/g, together with only 0.065% capacity fading per cycle (74% capacity retention). The structure stability of OPNS-72 after testing for 620 cycles was also confirmed by TEM analysis (Fig. \$18a). The morphology of OPNS-72 was largely preserved after the cycling tests, indicating that the flexible carbon chain in OPNS could effectively buffer the structural variation in the lithiation process. In addition, there was no peak corresponding to elemental sulfur observed in the XRD pattern of OPNS-72 after cycling (Fig. S18b), further confirming that the formation of elemental sulfur was avoided over cycling. Benefiting from the stable structure and high sulfur content, these well-designed materials demonstrated much better electrochemical performance than conventional organic polysulfanes and most of hybrid sulfur-based metal oxides/carbon composites in Li-S batteries [4,8,13,41-46]. The details are summarized in Table S1.

To further understand the lithium storage mechanism in the OPNS-72 electrode, we performed *in operando* Raman spectroscopy measurements at different stage of discharge and charge by slowly sweeping the cell voltage at a rate of 0.1 mV/s between 3.0 and 1.5 V (Fig. 4). The strong peak at 234 cm^{-1} in the Raman spectra could be attributed to LiNO₃, an additive agent in the electrolyte with high Raman activity [43]. During the discharge process (voltage decreased from 3.0 to

1.5 V), a number of new peaks located at wave number of 134, 182, 203, 287, 435, 497 and 650 cm $^{-1}$, corresponding to polysulfide of $\rm S_{1-8}^{2-}$ [23,47,48], appeared gradually in the Raman spectra. Besides, the peak intensities increased with the decreased voltage, indicating that the OPNS-72 was probably reduced to $\rm Li_2S_6$, $\rm Li_2S_4$, or $\rm Li_2S_{1-2}$ during the discharge process [12,49]. It was worth noting that during the charge process, the peak intensities of these polysulfides decreased gradually as the voltage increased from 2.4 to 3.0 V. All peaks disappeared when the charge process was completed (OCV 2.6 V), suggesting that lithium storage in the OPNS-72 electrode is highly reversible, which is crucial to long-term cycling stability.

4. Conclusions

In summary, a 2D organic polysulfane nanosheet with polycyclic sulfur grafted on the carbon chain of PAA has been rationally designed and successfully synthesized using a coupling reaction between elemental sulfur and PAA at 260 °C with KI as a catalyst and KCl as a template. The sulfur content can be tailored by adjusting the coupling reaction time. When tested as an electrode in a Li-S battery, the organic polysulfane with 72 wt% sulfur content (OPNS-72) demonstrated high specific capacity (e.g., 891 mAh/g at 1 C based on whole composite), excellent cycling life (capacity retention of over 91% after 620 cycles at 1 C), superior rate capability (retaining a specific capacity of 562 mAh/ g at 10 C) and high mass loading of 9.7 mg/cm². The TEM image of OPNS-72 after cycling test and In operando Raman spectroscopy analysis for OPNS-72 cathode indicate that both structure stability and reversible electrochemical reaction of the OPNS-72 electrode in the Li-S battery contribute to the high cycling stability. The as-developed organic polysulfane nanosheet is a promising cathode candidate for highperformance Li-S batteries. Further, this synthesis method is believed to be a general strategy applicable to synthesis of other 2D polymers and polymeric materials for Li-S batteries.

Acknowledgements

This work was supported by the US National Science Foundation under award number DMR-1410320 and DMR-1742828, the National Natural Science Foundation of China (Nos. 21573085 and 21377044), the Key Project of Natural Science Foundation of Hubei Province (No. 2015CFA037), and self-determined research funds of CCNU from the colleges' basic research and operation of MOE (No. CCNU18TS034). H. H. acknowledges the financial support of a scholarship from the China Scholarship Council (CSC).

Appendix A. Supplementary material

Supplementary data associated with this article can be found in the online version at doi:10.1016/j.nanoen.2018.12.092.

References

- A. Manthiram, Y. Fu, Y.-S. Su, Challenges and prospects of lithium-sulfur batteries, Acc. Chem. Res. 46 (2013) 1125–1134.
- [2] C.B. Bucur, J. Muldoon, A. Lita, A layer-by-layer supramolecular structure for a sulfur cathode, Energy Environ. Sci. 9 (2016) 992–998.
- [3] T. Tao, S. Lu, Y. Fan, W. Lei, S. Huang, Y. Chen, Anode improvement in rechargeable lithium-sulfur batteries, Adv. Mater. 29 (2017) 1700542.
- [4] W.J. Chung, J.J. Griebel, E.T. Kim, H. Yoon, A.G. Simmonds, H.J. Ji, P.T. Dirlam, R.S. Glass, J.J. Wie, N.A. Nguyen, B.W. Guralnick, J. Park, A. Somogyi, P. Theato, M.E. Mackay, Y.E. Sung, K. Char, J. Pyun, The use of elemental sulfur as an alternative feedstock for polymeric materials, Nat. Chem. 5 (2013) 518–524.
- [5] G. Li, J. Sun, W. Hou, S. Jiang, Y. Huang, J. Geng, Three-dimensional porous carbon composites containing high sulfur nanoparticle content for high-performance lithium-sulfur batteries, Nat. Commun. 7 (2016) 10601.
- [6] Z.W. Seh, W. Li, J.J. Cha, G. Zheng, Y. Yang, M.T. McDowell, P.C. Hsu, Y. Cui, Sulphur-TiO₂ yolk-shell nanoarchitecture with internal void space for long-cycle lithium-sulphur batteries, Nat. Commun. 4 (2013) 1331.
- [7] X. Liu, J.Q. Huang, Q. Zhang, L. Mai, Nanostructured metal oxides and sulfides for lithium-sulfur batteries, Adv. Mater. 29 (2017) 1601759.

[8] H. Kim, J. Lee, H. Ahn, O. Kim, M.J. Park, Synthesis of three-dimensionally interconnected sulfur-rich polymers for cathode materials of high-rate lithium-sulfur batteries, Nat. Commun. 6 (2015) 7278.

- [9] H.J. Peng, J.Q. Huang, Q. Zhang, A review of flexible lithium-sulfur and analogous alkali metal-chalcogen rechargeable batteries, Chem. Soc. Rev. 46 (2017) 5237–5288.
- [10] H. Hu, H. Cheng, Z. Liu, G. Li, Q. Zhu, Y. Yu, In situ polymerized PAN-assisted S/C nanosphere with enhanced high-power performance as cathode for lithium/sulfur batteries, Nano Lett. 15 (2015) 5116–5123.
- [11] Z. Sun, J. Zhang, L. Yin, G. Hu, R. Fang, H.-M. Cheng, F. Li, Conductive porous vanadium nitride/graphene composite as chemical anchor of polysulfides for lithium-sulfur batteries, Nat. Commun. 8 (2017) 14627.
- [12] A. Manthiram, Y. Fu, S.H. Chung, C. Zu, Y.S. Su, Rechargeable lithium-sulfur batteries, Chem. Rev. 114 (2014) 11751–11787.
- [13] G. Hu, Z. Sun, C. Shi, R. Fang, J. Chen, P. Hou, C. Liu, H.M. Cheng, F. Li, A sulfurrich copolymer@ CNT hybrid cathode with dual-confinement of polysulfides for high-performance lithium-sulfur batteries, Adv. Mater. 29 (2017) 1603835.
- [14] F. Wu, S. Chen, V. Srot, Y. Huang, S.K. Sinha, P.A. van Aken, J. Maier, Y. Yu, A sulfur-limonene-based electrode for lithium-sulfur batteries: high-performance by self-protection, Adv. Mater. 30 (2018) 1706643.
- [15] J. Liu, M. Wang, N. Xu, T. Qian, C. Yan, Progress and perspective of organosulfur polymers as cathode materials for advanced lithium-sulfur batteries, Energy Storage Mater. 15 (2018) 53–64.
- [16] R. Steudel, The chemistry of organic polysulfanes R-Sn-R (n > 2), Chem. Rev. 102 (2002) 3905–3946.
- [17] A.G. Simmonds, J.J. Griebel, J. Park, K.R. Kim, W.J. Chung, V.P. Oleshko, J. Kim, E.T. Kim, R.S. Glass, C.L. Soles, Y.-E. Sung, K. Char, J. Pyun, Inverse vulcanization of elemental sulfur to prepare polymeric electrode materials for Li-S batteries, ACS Macro Lett. 3 (2014) 229–232.
- [18] J. Zhou, T. Qian, N. Xu, M. Wang, X. Ni, X. Liu, X. Shen, C. Yan, Selenium-doped cathodes for lithium-organosulfur batteries with greatly improved volumetric capacity and coulombic efficiency, Adv. Mater. 29 (2017) 1701294.
- [19] I.P. Beletskaya, V.P. Ananikov, Transition-metal-catalyzed C-S, C-Se, and C-Te bond formation via cross-coupling and atom-economic addition reactions, Chem. Rev. 111 (2011) 1596–1636.
- [20] K.L. Dunbar, D.H. Scharf, A. Litomska, C. Hertweck, Enzymatic carbon-sulfur bond formation in natural product biosynthesis, Chem. Rev. 117 (2017) 5521–5577.
- [21] D. Chen, J.-H. Wang, T.-F. Chou, B. Zhao, M.A. El-Sayed, M. Liu, Unraveling the nature of anomalously fast energy storage in T-Nb₂O₅, J. Am. Chem. Soc. 139 (2017) 7071–7081.
- [22] X. Xiao, H. Song, S. Lin, Y. Zhou, X. Zhan, Z. Hu, Q. Zhang, J. Sun, B. Yang, T. Li, L. Jiao, J. Zhou, J. Tang, Y. Gogotsi, Scalable salt-templated synthesis of two-dimensional transition metal oxides. Nat. Commun. 7 (2016) 11296.
- [23] J.-J. Chen, R.-M. Yuan, J.-M. Feng, Q. Zhang, J.-X. Huang, G. Fu, M.-S. Zheng, B. Ren, Q.-F. Dong, Conductive lewis base matrix to recover the missing link of Li₂S₈ during the sulfur redox cycle in Li-S battery, Chem. Mater. 27 (2015) 2048–2055.
- [24] L. Xiao, Y. Cao, J. Xiao, B. Schwenzer, M.H. Engelhard, L.V. Saraf, Z. Nie, G.J. Exarhos, J. Liu, A soft approach to encapsulate sulfur: polyaniline nanotubes for lithium-sulfur batteries with long cycle life, Adv. Mater. 24 (2012) 1176–1181.
 [25] G. Xu, A. Kushima, J. Yuan, H. Dou, W. Xue, X. Zhang, X. Yan, J. Li, Ad hoc solid
- [25] G. Xu, A. Kushima, J. Yuan, H. Dou, W. Xue, X. Zhang, X. Yan, J. Li, Ad hoc solid electrolyte on acidized carbon nanotube paper improves cycle life of lithium-sulfur batteries, Energy Environ. Sci. 10 (2017) 2544–2551.
- [26] B.-C. Yu, J.-W. Jung, K. Park, J.B. Goodenough, A new approach for recycling waste rubber products in Li-S batteries, Energy Environ. Sci. 10 (2017) 86–90.
- [27] X. Wang, J. Wang, D. Wang, S. Dou, Z. Ma, J. Wu, L. Tao, A. Shen, C. Ouyang, Q. Liu, S. Wang, One-pot synthesis of nitrogen and sulfur co-doped graphene as efficient metal-free electrocatalysts for the oxygen reduction reaction, Chem. Commun. 50 (2014) 4839–4842.
- [28] R. Steudel, Inorganic polysulfides $\rm S_n^{\,2-}$ and radical anions $\rm S_n^{\,-}$, Top. Curr. Chem. 231 (2003) 127–152.
- [29] Y. Yang, J. Liu, Z.W. Fu, D. Qin, Galvanic replacement-free deposition of Au on Ag for core-shell nanocubes with enhanced chemical stability and SERS activity, J. Am. Chem. Soc. 136 (2014) 8153–8156.
- [30] J.M. McLellan, Z.-Y. Li, A.R. Siekkinen, Y. Xia, The SERS activity of a supported Ag nanocube strongly depends on its orientation relative to laser polarization, Nano Lett. 7 (2007) 1013–1017.
- [31] J. Dong, Y. Ozaki, K. Nakashima, Infrared, Raman, and Near-Infrared spectroscopic evidence for the coexistence of various hydrogen-bond forms in poly(acrylic acid), Macromolecules 30 (1997) 1111–1117.
- [32] S.W. Cornell, J.L. Koenig, The raman spectra of polybutadiene rubbers, Macroniolecules 2 (1969) 540–545.
- [33] Y. Jin, G. Zhou, F. Shi, D. Zhuo, J. Zhao, K. Liu, Y. Liu, C. Zu, W. Chen, R. Zhang, X. Huang, Y. Cui, Reactivation of dead sulfide species in lithium polysulfide flow battery for grid scale energy storage, Nat. Commun. 8 (2017) 462.
- [34] H. Hu, H. Cheng, G. Li, J. Liu, Y. Yu, Design of SnO₂/C hybrid triple-layer nanospheres as Li-ion battery anodes with high stability and rate capability, J. Mater. Chem. A 3 (2015) 2748–2755.
- [35] G. Hu, C. Xu, Z. Sun, S. Wang, H.M. Cheng, F. Li, W. Ren, 3D graphene-foam-reduced-graphene-oxide hybrid nested hierarchical networks for high-performance Li-S batteries, Adv. Mater. 28 (2016) 1603–1609.
- [36] L. Li, T.A. Pascal, J.G. Connell, F.Y. Fan, S.M. Meckler, L. Ma, Y.M. Chiang, D. Prendergast, B.A. Helms, Molecular understanding of polyelectrolyte binders that actively regulate ion transport in sulfur cathodes, Nat. Commun. 8 (2017) 2277
- [37] T. Zhou, W. Lv, J. Li, G. Zhou, Y. Zhao, S. Fan, B. Liu, B. Li, F. Kang, Q.-H. Yang, Twinborn TiO₂-TiN heterostructures enabling smooth trapping-diffusion-

- conversion of polysulfides towards ultralong life lithium-sulfur batteries, Energy Environ. Sci. $10\ (2017)\ 1694-1703$.
- [38] B. Wang, S.M. Alhassan, S.T. Pantelides, Formation of large polysulfide complexes during the lithium-sulfur battery discharge, Phys. Rev. Appl. 2 (2014) 034004.
- [39] Z. Yang, Z. Zhu, J. Ma, D. Xiao, X. Kui, Y. Yao, R. Yu, X. Wei, L. Gu, Y.-S. Hu, H. Li, X. Zhang, Phase separation of Li₂S/S at nanoscale during electrochemical lithiation of the solid-state lithium-sulfur battery using in situ TEM, Adv. Energy Mater. 6 (2016) 1600806.
- [40] Y. Yang, G. Zheng, S. Misra, J. Nelson, M.F. Toney, Y. Cui, High-capacity micrometer-sized Li₂S particles as cathode materials for advanced rechargeable lithium-ion batteries, J. Am. Chem. Soc. 134 (2012) 15387–15394.
- [41] J. Zhang, Y. Shi, Y. Ding, W. Zhang, G. Yu, In situ reactive synthesis of polypyrrole-MnO₂ coaxial nanotubes as sulfur hosts for high-performance lithium-sulfur battery, Nano Lett. 16 (2016) 7276–7281.
- [42] J. Liu, T. Qian, M. Wang, X. Liu, N. Xu, Y. You, C. Yan, Molecularly imprinted polymer enables high-efficiency recognition and trapping lithium polysulfides for stable lithium sulfur battery, Nano Lett. 17 (2017) 5064–5070.
- [43] M. Yu, J. Ma, H. Song, A. Wang, F. Tian, Y. Wang, H. Qiu, R. Wang, Atomic layer deposited TiO₂ on a nitrogen-doped graphene/sulfur electrode for high performance lithium-sulfur batteries, Energy Environ. Sci. 9 (2016) 1495–1503.
- [44] J. Zhang, C.P. Yang, Y.X. Yin, L.J. Wan, Y.G. Guo, Sulfur encapsulated in graphitic carbon nanocages for high-rate and long-cycle lithium-sulfur batteries, Adv. Mater. 28 (2016) 9539–9544.
- [45] Z. Li, J. Zhang, B. Guan, D. Wang, L.M. Liu, X.W. Lou, A sulfur host based on titanium monoxide@ carbon hollow spheres for advanced lithium-sulfur batteries, Nat. Commun. 7 (2016) 13065.
- [46] Z. Li, J.T. Zhang, Y.M. Chen, J. Li, X.W. Lou, Pie-like electrode design for high-energy density lithium-sulfur batteries, Nat. Commun. 6 (2015) 8850.
- [47] H.L. Wu, L.A. Huff, A.A. Gewirth, In situ Raman spectroscopy of sulfur speciation in lithium-sulfur batteries, ACS Appl. Mater. Interfaces 7 (2015) 1709–1719.
- [48] M. Hagen, P. Schiffels, M. Hammer, S. Dörfler, J. Tübke, M.J. Hoffmann, H. Althues, S. Kaskel, In-situ raman investigation of polysulfide formation in Li-S cells, J. Electrochem. Soc. 160 (2013) (A1205-A1204).
- [49] R. Fang, S. Zhao, Z. Sun, D.W. Wang, H.M. Cheng, F. Li, More reliable lithium-sulfur batteries: status, solutions and prospects, Adv. Mater. 29 (2017) 1606823.



Hao Hu received his double Bachelor's degree in Physics and Applied Chemistry at Central China Normal University in 2012. He is currently pursuing his Ph.D. under the supervision of Prof. Ying Yu in the Institute of Nano-Science and Nano-Technology at Central China Normal University. He joined Prof. Meilin Liu's group as a joint Ph.D. student at School of Materials Science and Engineering, Georgia Institute of Technology in November 2016. His research interests mainly focus on the efficient energy storage and conversion, including supercapacitors, metal ion batteries and interface electrochemistry.



Haoyan Cheng received her Bachelor's degree in physics from Luoyang Normal University in 2012. She is pursuing her Ph.D. degree in the Institute of Nano-Science and Nano-Technology at Central China Normal University. She joined the Younan Xia's group as a visiting student in November 2016. Currently, her research interest includes fabrication of nanomaterials with controlled shapes and compositions for the application in nanomedicine and fuel cells.



Bote Zhao is currently a post-doctoral fellow at the School of Materials Science and Engineering at Georgia Institute of Technology, USA. He received his B.S. and Ph.D. from Nanjing Tech University, China. He is currently focusing on the rational design, synthesis and characterization of novel materials for electrocatalysis, batteries, fuel cells, and supercapacitors. He has been recognised as one of Top 10 Outstanding Reviewers for Journal of Materials Chemistry A in 2016 & 2017.



Shuge Dai is currently an associate professor at School of Physics and Engineering, Zhengzhou University. He received his Ph.D degree from the Department of Applied Physics at Chongqing University of China. He joined Prof. Meilin Liu's group as a visiting student at School of Materials Science and Engineering, Georgia Institute of Technology in 2015. His research interests mainly focus on the efficient energy storage and conversion, including supercapacitors, nanogenerators, and lithium ion batteries.



Nicholas Kane received his Bachelor's degree in Materials Science & Engineering from the Georgia Institute of Technology and is currently a pursuing his Ph.D. there under the supervision of Prof. Meilin Liu. His research experiences include binder-free electrodes, nanostructured materials for lithium ion batteries and supercapacitors, and electrospinning synthesis of fibers. His current research focuses on the development of model cells allowing for institu observation of electrode surfaces, as well as the fabrication of thin film catalyst coatings



Ying Yu is currently a professor in College of Physical Science and Technology at Central China Normal University, China. She received her Ph.D. degree in Environmental Science from Nankai University in 2000. Her research mainly focuses on unique design of efficient nanomaterials for $\rm CO_2/N_2$ reduction, water splitting and pollutants degradation; nanostructured materials for energy storage; DFT calculations based on photocatalysis and electrocatalysis.



Meilin Liu is a B. Mifflin Hood Chair, Regents' Professor, and Associate Chair of Materials Science and Engineering and Co-Director of the Center for Innovative Fuel Cell and Battery Technologies at Georgia Institute of Technology, Atlanta, Georgia, USA. He received his BS from South China University of Technology and both MS and Ph.D. from University of California at Berkeley. His research interests include insitu/operando characterization and multi-scale modeling of charge and mass transfer along surfaces, across interfaces, and in membranes, thin films, and nanostructured electrodes, aiming at achieving rational design of materials and structures with unique functionalities for efficient energy storage and conversion.